

Iranian Journal of Oil & Gas Science and Technology, Vol. 10 (2021), No. 4, pp. 14–30
<http://ijogst.put.ac.ir>

Sensor Fault Diagnosis Using an Algorithm Based on Auto-Associative Neural Networks

Hamidreza Mousavi¹ and Mehdi Shahbazian^{2*}

¹ M.S. Student, Department of Instrumentation and Automation Engineering, Petroleum University of Technology, Ahwaz, Iran.

² Associate Professor, Department of Instrumentation and Automation Engineering, Petroleum University of Technology, Ahwaz, Iran.

Highlights

- An algorithm named improved auto-associative neural network (I-AANN) is presented for sensor fault diagnosis;
- The algorithm uses a calibration model based on auto-associative neural network (AANN);
- The I-AANN performance is compared with enhanced auto-associative neural network (E-AANN);
- The algorithm is a kind of nonlinear principal component analysis (NLPCA);
- The algorithm can detect and isolate faulty sensors via reconstruction;
- Due to the low computational time, the algorithm is capable of online application.

Received: July 08, 2021; revised: October 22, 2021; accepted: November 05, 2021

Abstract

Auto-associative neural network (AANN) has been recently used in sensor fault diagnosis. This paper introduces a new AANN based algorithm named improved AANN (I-AANN) for sensor single-fault diagnosis. An algorithm is a two-aimed approach that estimates the correct value of the faulty sensor by isolating the source of the fault. The performance of the algorithm is compared with the so-called enhanced AANN (E-AANN) in terms of computational time and fault reconstruction accuracy. The I-AANN has high performance, and it can isolate the source of fault quickly and accurately. A dimerization process model is used as a case study to examine and compare the performance of the algorithms. The results demonstrate that the I-AANN has superior performance.

Keywords: Auto-associative neural networks; Reconstruction algorithm; Sensor fault diagnosis

How to cite this article

Mousavi, H. R. and Shahbazian, M., Sensor Fault Diagnosis Using an Algorithm Based on Auto-Associative Neural Networks, Iran J. Oil Gas Sci. Technol., Vol. 10, No. 4, pp. 14–30, 2021.

DOI: <http://dx.doi.org/10.22050/ijogst.2021.293463.1606>, This is an Open Access article under Creative Commons Attribution 4.0 International License.(creativecommons.org/licenses/by/4.0/)



1. Introduction

Process history-based approaches to fault diagnosis have been widely used recently. In contrast to model-based methods, which need knowledge about the process, they only need a large amount of historical process data (Venkatasubramanian et al., 2003). Most historical process data source from the

* Corresponding author:

Email: m.shahbazian@put.ac.ir

process sensors, which are integral to control systems. The sensor measurements must be reliable in a control system because when sensors become faulty, the system will be unreliable (Sing, 2004). If one of the sensors becomes faulty, the decision based on the faulty data set likely leads to incorrect control actions and may shut the process down. Sensor fault diagnosis is a subset of process monitoring and fault diagnosis (Najafi et al., 2004).

By introducing redundant sensors, data redundancy is typically produced, so data needed for the fault-tolerant control algorithm is supplied. Two redundant sensors are enough for detecting a fault, but more sensors are required to locate a faulty sensor. However, due to the cost of the extra sensors, increasing the number of sensors and their maintenance become expensive, which may also impose additional duty on control software and hardware. Sensor fault diagnosis focuses on finding the dysfunctional sensors (Najafi, 2003).

Auto-associative neural network (AANN) is an approach widely used for sensor fault diagnosis. When one of the AANN inputs is contaminated or degraded because of the inherent non-orthogonality of the AANN, it affects all the outputs of the auto-associative neural network. Hence, traditional methods like contribution plots and Hine's approach are not reliable for fault isolation (Najafi, 2003). This paper introduces a reconstruction-based algorithm for sensor fault detection and isolation (FDI) named improved auto-associative neural network (I-AANN). The algorithm performance is compared with the performance of the recently developed algorithm, i.e., enhanced auto-associative neural network (E-AANN), (Najafi et al., 2003, 2004). The I-AANN uses a new and better search method than the E-AANN, representing better performance. The main objective of this paper is to introduce the I-AANN algorithm and compare its performance with the E-AANN. To this end, a dimerization plant model was used to generate the plant input and output data to examine the algorithms.

The paper contains seven sections: Section 2 explains the AANN, and Section 3 presents the E-AANN algorithm. The I-AANN algorithm is presented in Section 4, and the application study is described in Section 5. The results and discussion are presented in Section 6, and Section 7 summarizes the paper.

2. Auto-associative neural networks

Auto-associative neural network developed by Kramer (1991) is widely used for sensor fault diagnosis. Training the AANN can capture the interrelation between the process variables in its weights, and the process variables should have some degree of correlation with each other. The outputs are trained in AANN for emulating the inputs over an appropriate dynamic range (Kramer, 1991). An AANN consists of mapping, bottlenecking, and demapping layers in addition to one input and one output layer. A three-hidden-layer AANN architecture is shown in Figure 1.

In all hidden layers, the activation functions are the sigmoidal function:

$$\sigma(x) = 1/(1 + \exp(-x)) \quad (1)$$

On the basis of the least-squares sense, the AANN is trained so that its outputs match the inputs as closely as possible over the training set. When data without faulty sensors are fed to the trained AANN, the difference between the input and output of the AANN algorithm is ideally zero. If one or more sensors are faulty, that is, the data are contaminated, the difference between the input and output of the AANN algorithm will be nonzero.

The AANN is the heart of the reconstructing algorithms used for sensor single-fault isolation. The following two sections explain the algorithms.

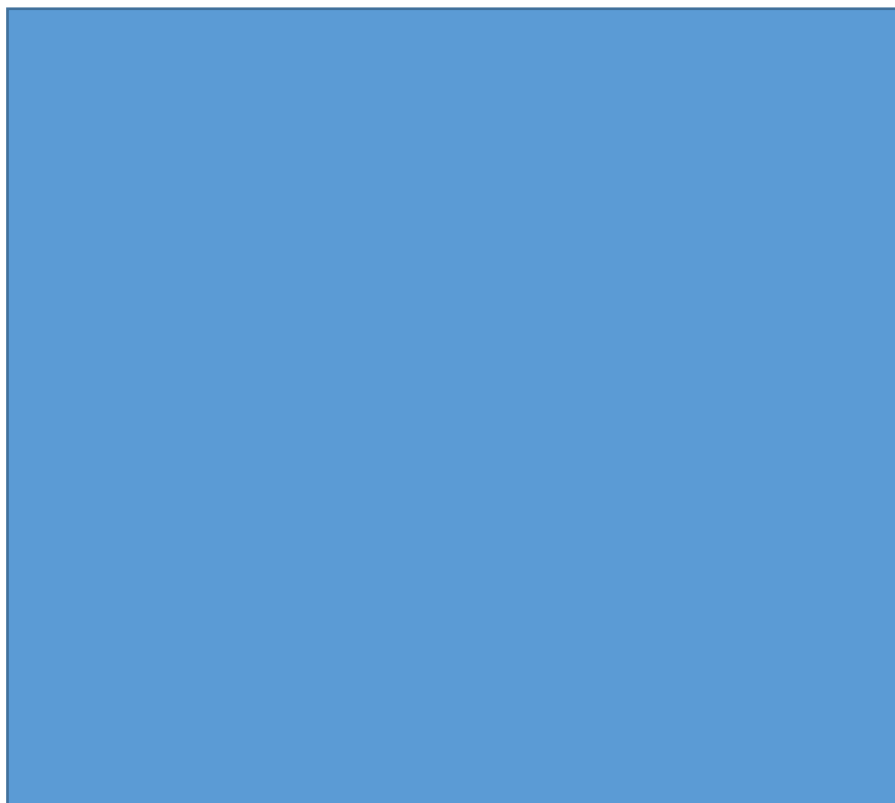


Figure 1

The structure of auto-associative neural network (Najafi et al., 2004).

3. Enhanced AANN

An extension of the AANN is the enhanced auto-associative neural network introduced by Najafi et al. (2003 and 2004), which is applied to the detection and isolation of a single faulty sensor. The E-AANN can detect one faulty sensor at most and uses a simple search algorithm. The algorithm uses a simple linear search strategy to find the global minimum of an objective function defined by the AANN via searching through the whole search space. The input of the E-AANN is both the output measured data and the input of the process. The E-AANN output is reconstructed data. If there is no fault in the input data, the difference between the input and output of the E-AANN will be zero, and the E-AANN output will be the same as the input. If one of the inputs does not have an expected value, the difference in the corresponding output will be nonzero (Sing, 2004; Najafi et al., 2004).

The E-AANN reconstruction algorithm searches from the minimum to maximum value of sensors with a predefined step size and detects and isolates the occurred fault simultaneously. In order to find the location of the faulty sensor, all inputs are held fixed, and one of the inputs is changed over its defined range to determine when the sum of squared error (SSE) is zero or close to zero (minimized). Once the SSE becomes zero, the corresponding sensor is identified as faulty. Selecting the step size is a crucial parameter in the algorithm; indeed, the higher the magnitude of the step size is, the shorter the computation time becomes. On the other hand, the smaller the magnitude of the step size is, the more accurate the results are. Therefore, the computational time is raised if we select a small step size, which is a disadvantage because, for fast processes, the computational time is very crucial. Further, if we select a high magnitude step size, the accuracy of the results is low, and the algorithm cannot reconstruct and isolate the faulty sensor properly. Our simulation results demonstrates that the step size should be selected low enough, so the computational time for the E-AANN becomes considerable. Hence, we introduce an improved AANN algorithm to remedy this problem.

4. Improved AANN

The proposed I-AANN fault processing approach consists of two steps: detection and isolation. The detection step determines if there is any fault in the system. Usually, in statistical process monitoring (SPM), fault detection is done using generated residuals. This paper especially employs the residuals of the AANN, which define squared prediction error (SPE), for fault detection because the SPE may have lower changes for giving false alarms in process monitoring (Khaled, 2010; Borgan, 2011). After the fault detection step, the isolation part locates the faulty sensor if the system is faulty. The isolation step searches numerically from the minimum to maximum value of the sensors to find the global minimum of the objective function. The proposed I-AANN searching procedure is new and different from the E-AANN. The I-AANN searches by a high step size first and then focuses on the global minimum interval. This interval is searched with a low step size. Therefore, the computational time is decreased while the accuracy is increased. In addition, the isolation part analyzes the faulty samples determined in the detection part.

The computational time decreases because the algorithm focuses on searching in a small interval rather than the whole interval, the detection part determines the faulty samples, and fault isolation is done only for the faulty samples. The accuracy also increases because the small interval is searched with a smaller step size.

5. Case study

A dimerization model, an open-loop process, is used to compare the performance of E-AANN with I-AANN. Producing butene-1 is the catalytic dimerization of ethylene and is one of the most economical methods. The reactor of the industrial ethylene dimerization operates at bubble point under liquid phase conditions. A continuous feed of the reactor is a mixture of the homogenous catalyst and fresh ethylene, where an external cooler is used to remove the heat of the exothermic reaction. The location of the cooler is on the recycle pipelines. A portion of the product is recycled and returned to the reactor. High nonlinearity is the characteristic of this ethylene dimerization process. On the basis of industrial experience, regular and exact monitoring of the process variables is necessary (Ali and Al-humaizi, 2004). Because of using measured values for the process control, measuring instruments and sensors are very important in this process; regular monitoring and maintenance are also needed because they should be reliable. The process is performed in a continuous stirred tank reactor (CSTR). Figure 2 shows an exemplary schematic of this process.

**Figure 2**

The dimerization reaction process (Ali and Al-humaizi, 2004).

The process has seven variables for monitoring: the reactor temperature (T), the feed temperature (T_f), the concentration of catalyst in the feed (A_k), the feed flow rate (Fe), the recycle ratio (β), the coolant flow rate (Wc), and the produced butene concentration (Bc). We use the MATLAB SIMULINK model of the process for data generation.

5.1. Data generation

About 2000 sample data were generated using the dimerization process model. Seven variables were included in each data set sample, introduced in the above section. About 1% white noise was induced to the data set to simulate the actual situation. The data set was first normalized and then randomized. After that, a set of 1500 samples were selected randomly for training the AANN, and the remaining 500 samples were used as the testing set. Two types of faults (drift and shift) were introduced to the test data set for testing the algorithms.

6. Results and discussion

A drift fault is a kind of sensor fault in which the sensor error takes place slowly and incrementally. The error is minimal initially but grows gradually with time in this fault. Shift fault is another kind of sensor error happening suddenly (Najafi, 2003).

The normalized training and testing sets are depicted in Figures 3 and 4, respectively.

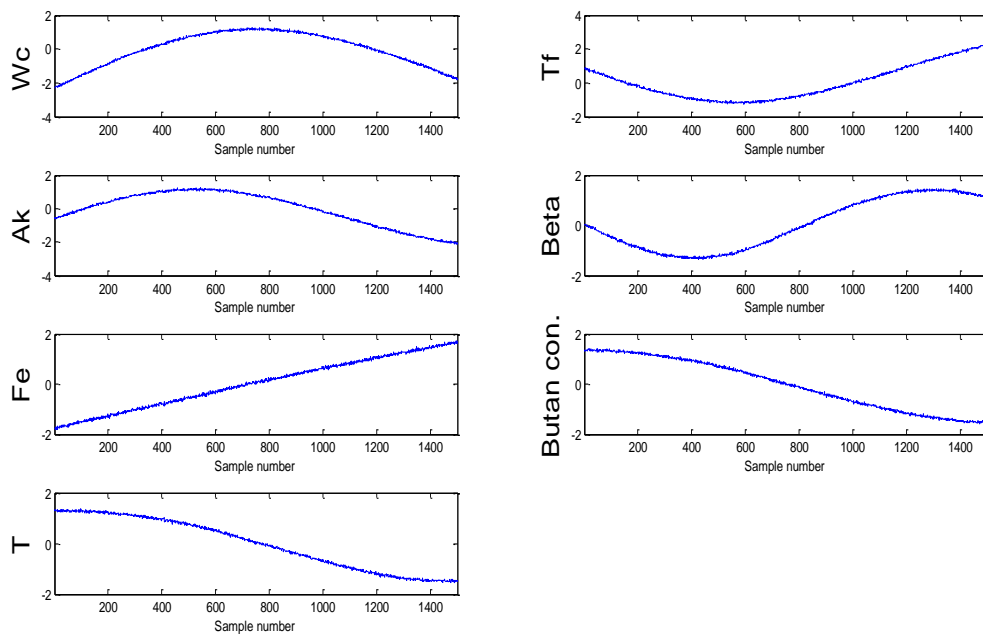


Figure 3
The normalized training set (sorted).

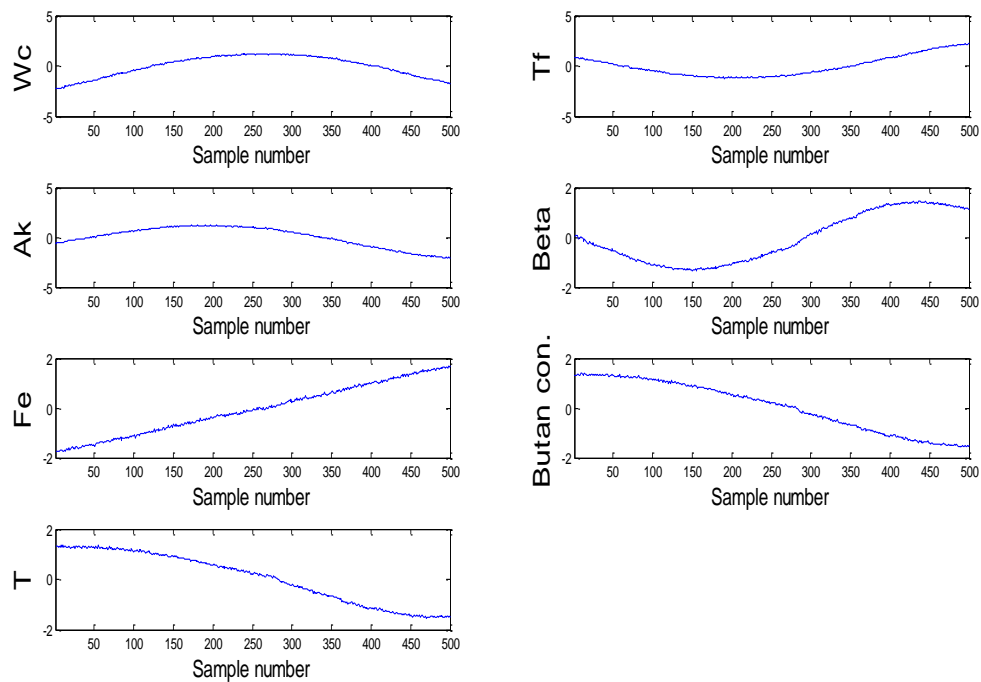


Figure 4
The normalized testing set (sorted).

Sensor number 7 is a thermocouple for measuring the temperature of the process product and is selected for applying a shift error of 10% (see Figure 5). The fault duration is from sample 200 to sample 400.

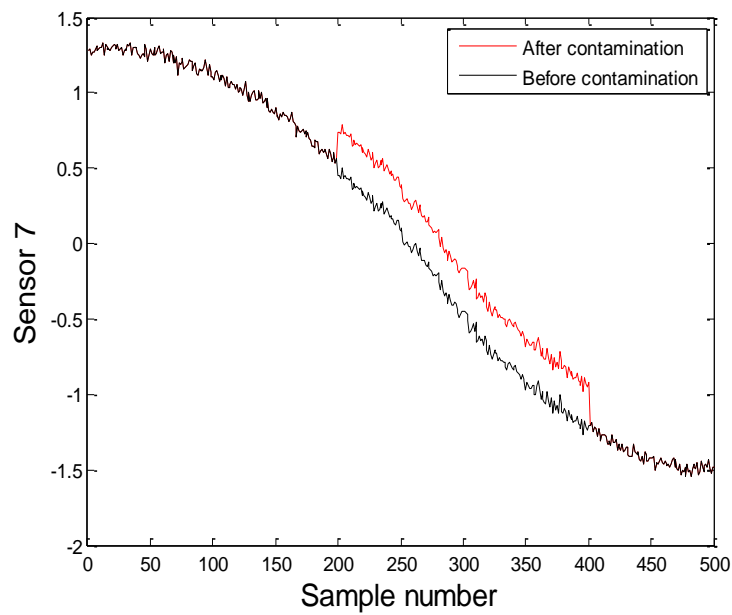


Figure 5

Sensor 7 output before and after contamination (shift fault).

The AANN structure for the algorithms is decided to be 7-10-3-10-7, and the training algorithm is selected to be scaled conjugate gradient (Scg). The E-AANN output for sensor 7 is shown in Figure 6.

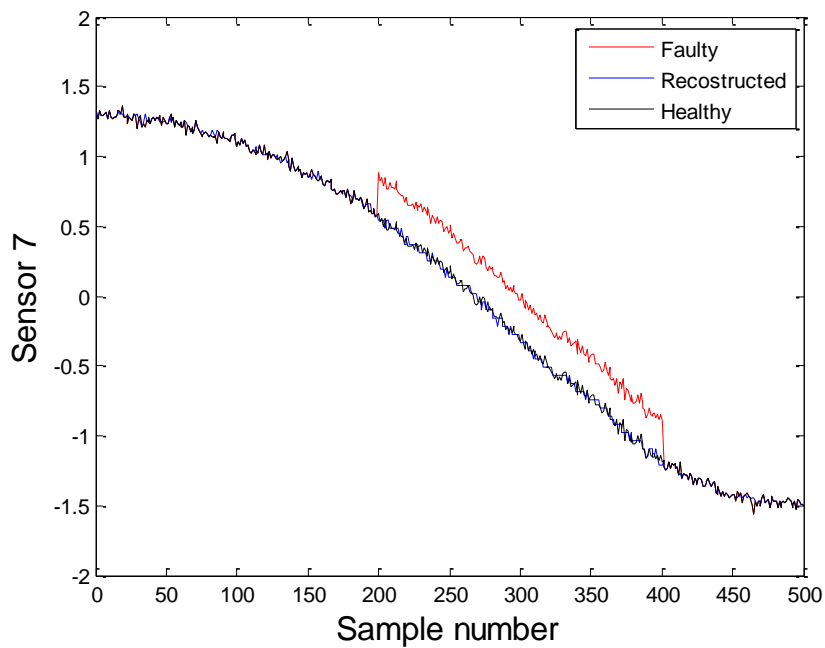
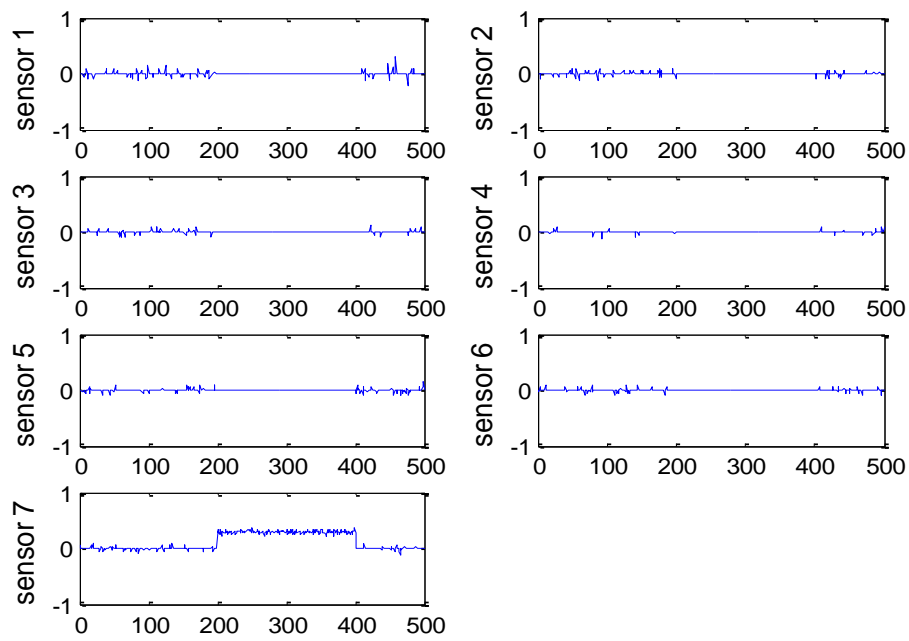


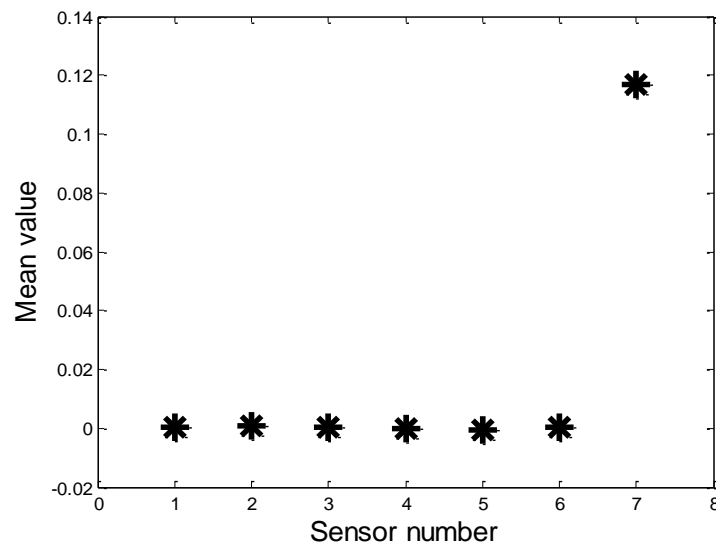
Figure 6

Sensor 7 output before contamination, after inducing a shift error, and after reconstruction by the E-AANN.

Figures 7 and 8 delineate the error of the E-AANN and the mean error, respectively.

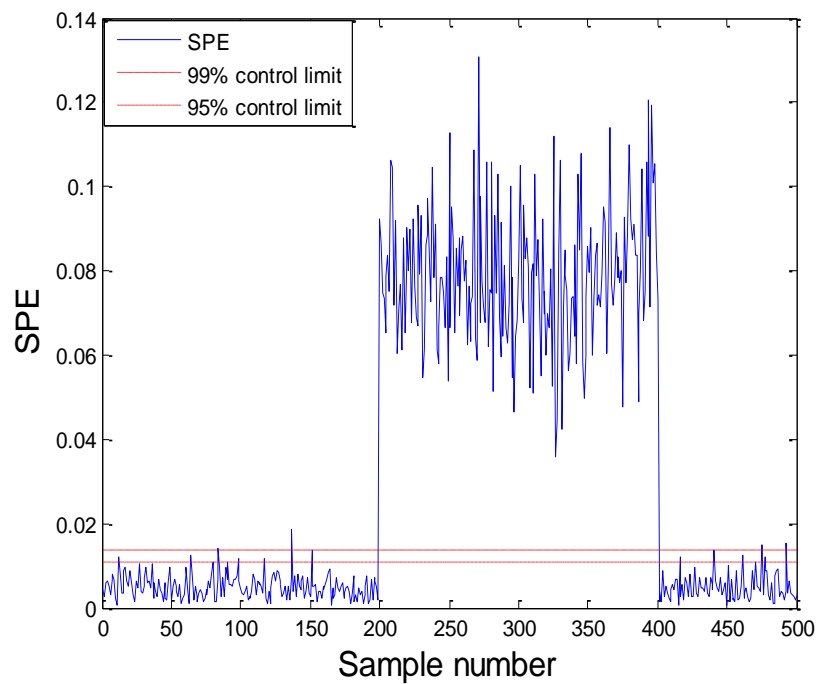
**Figure 7**

The difference between the E-AANN input and output; the input data had a shift error.

**Figure 8**

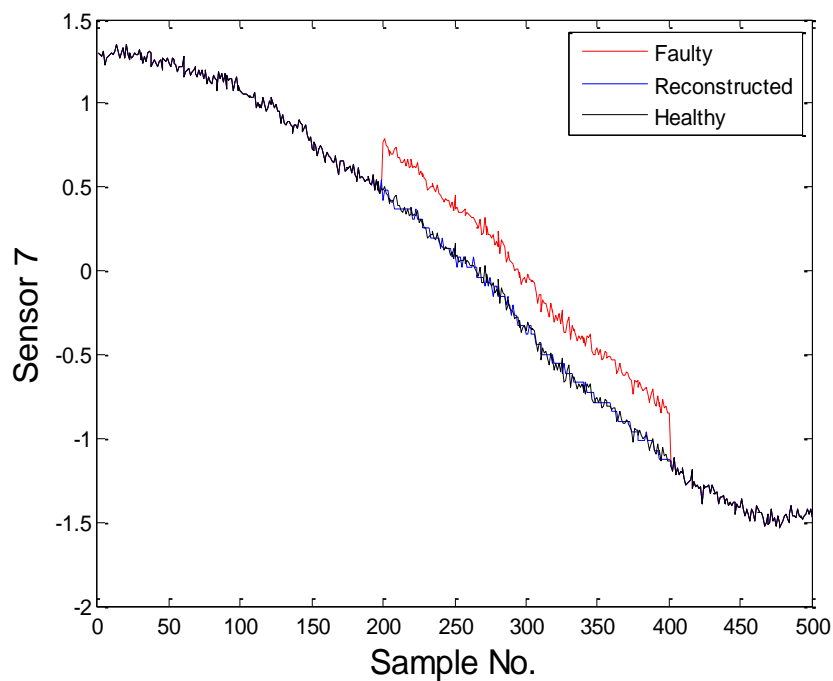
The mean of the difference between the input and output of the E-AANN for a shift fault.

Figure 9 shows the result of the detection part of the I-AANN. The process is faulty between samples 200 to 400, so the isolation part is implemented.

**Figure 9**

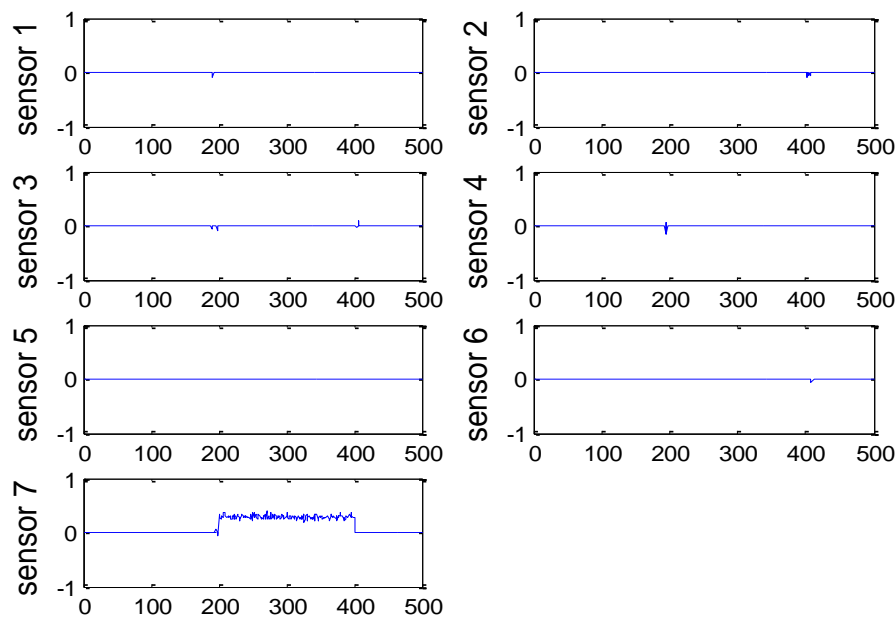
The shift fault detection by the I-AANN.

The I-AANN output for sensor 7 is shown in Figure 10.

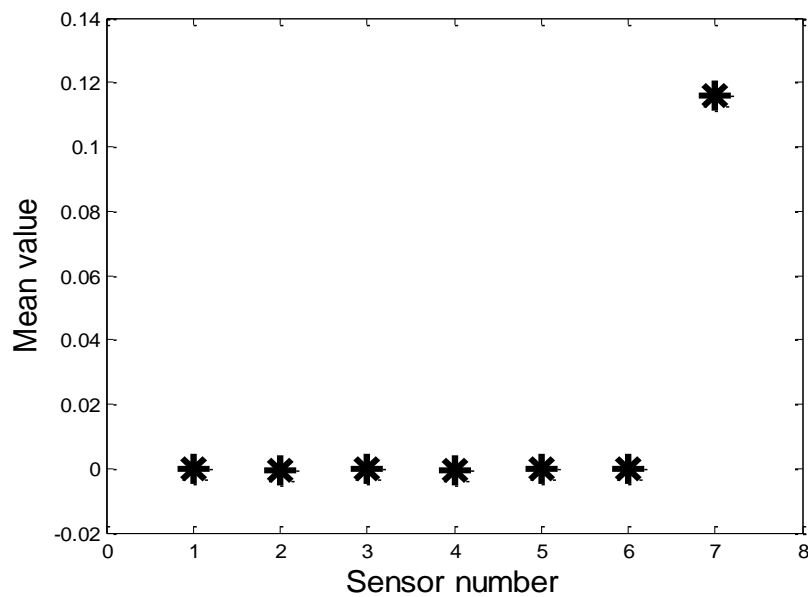
**Figure 8**

Sensor 7 output before contamination, after inducing a shift error, and after reconstruction by the I-AANN.

Figures 11 and 12 show the error of the I-AANN and the mean error, respectively.

**Figure 11**

The difference between the I-AANN input and output; the input data had a shift error.

**Figure 12**

The mean of the difference between the input and output of the I-AANN for a shift fault.

The error and mean of the error for the algorithms show that sensor 7 is the faulty sensor. Although both algorithms have isolated the faulty sensor, they have different performances.

Two critical parameters affecting the performance of each reconstruction algorithm are computational time and accuracy of the reconstruction. Tables 1 and 2 present the computational time and accuracy, respectively, to compare the performance of the algorithms. Two algorithms have the same step size.

Table 1

Comparing the reconstruction computational time (shift fault).

Reconstruction algorithm	E-AANN	I-AANN
Total computational time for 500 samples (s)	1215.9	233.6618
Computational time per sample (s)	2.4319	0.4673

The sum of squared error value for each algorithm is listed in Table 2.

Table 2

Comparing the accuracy of the reconstruction algorithms (shift fault) via the SSE.

Sensor 7	The E-AANN Output	The I-AANN Output
SSE	0.6083	0.0204

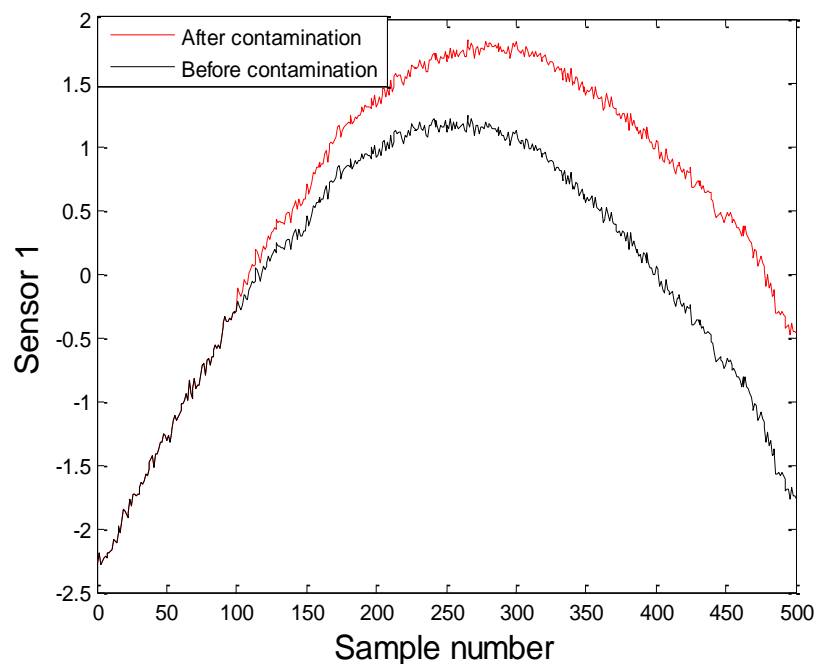
The I-AANN algorithm has a shorter computational time and higher accuracy than the E-AANN algorithm. Table 3 compares the performance of the E-AANN and I-AANN algorithms with approximately the same computational time for a random sample. The correct value for sensor 7 in the random sample is -0.7685 .

Table 3

The accuracy of the E-AANN and I-AANN at the same computational time.

Reconstruction algorithm	E-AANN	I-AANN
Computational time per sample (s)	0.4578	0.4673
Sensor 7 value (Correct value: -0.768)	-0.5832	-0.7388
Deviation from correct value	0.1848	0.0292

For the same computational time, the I-AANN has a higher degree of accuracy than the E-AANN. Another fault type is the drift error. Sensor number 1, an orifice plate measuring the flow rate of the coolant, is contaminated with a drift fault (Figure 13). The fault duration is from sample 100 to sample 500.

**Figure 13**

Sensor 1 output before and after contamination.

The results of the E-AANN are presented in Figures 14–16.

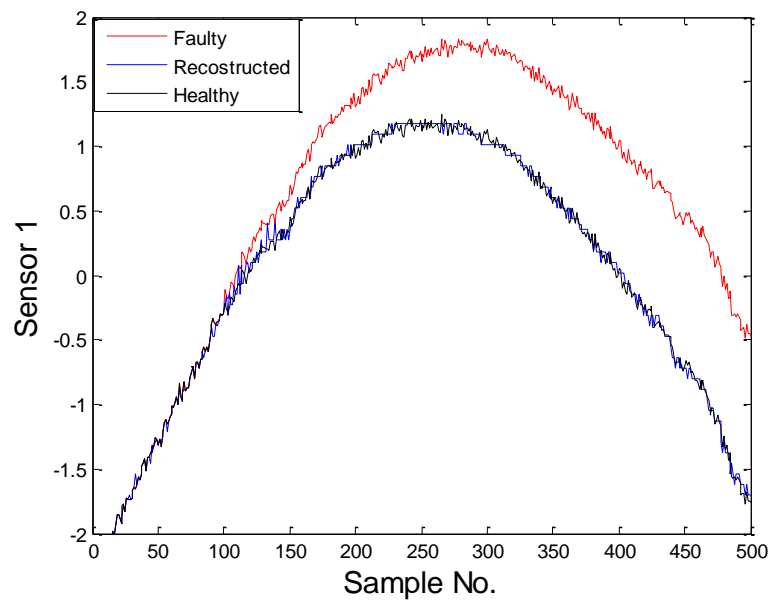


Figure 14

Sensor 1 output before contamination, after inducing a drift error, and after the reconstruction by the E-AANN.

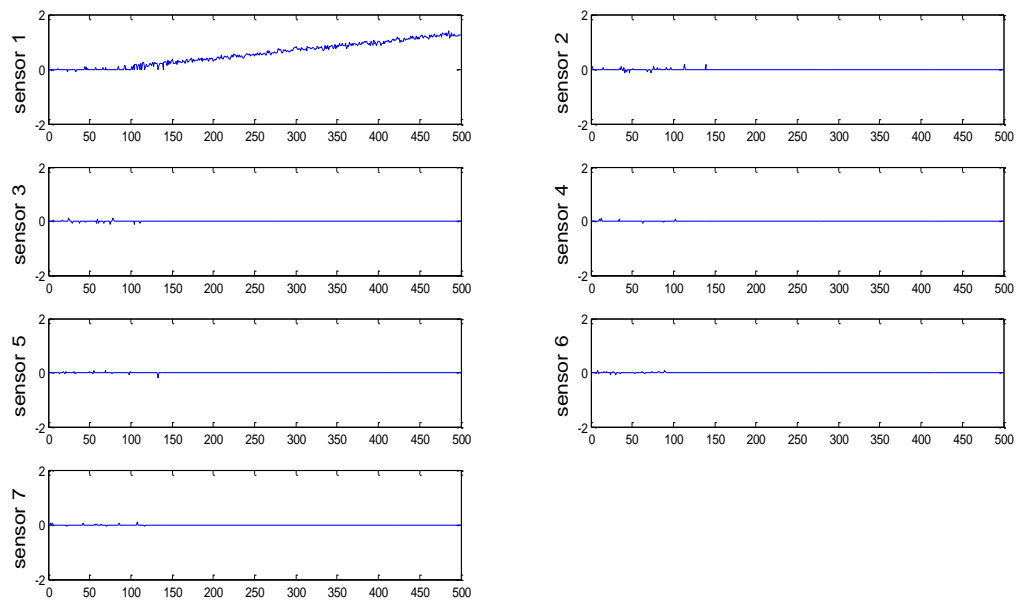
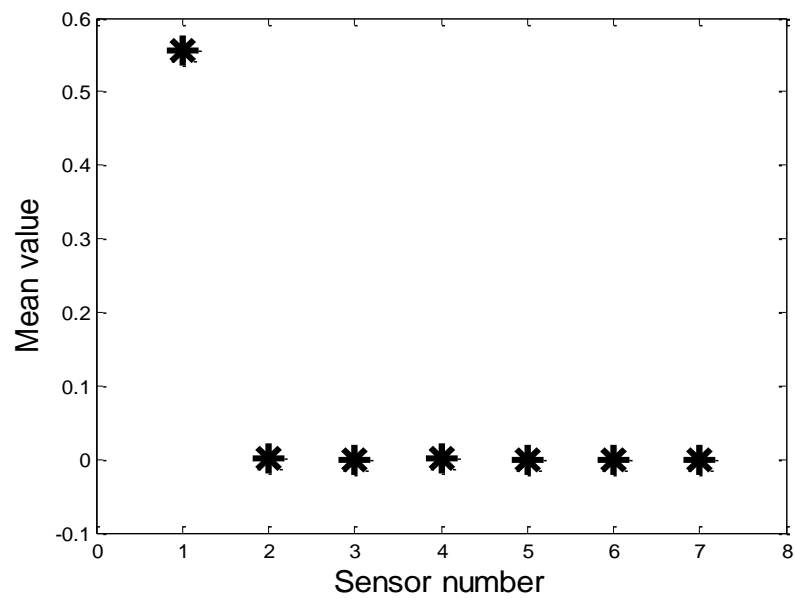


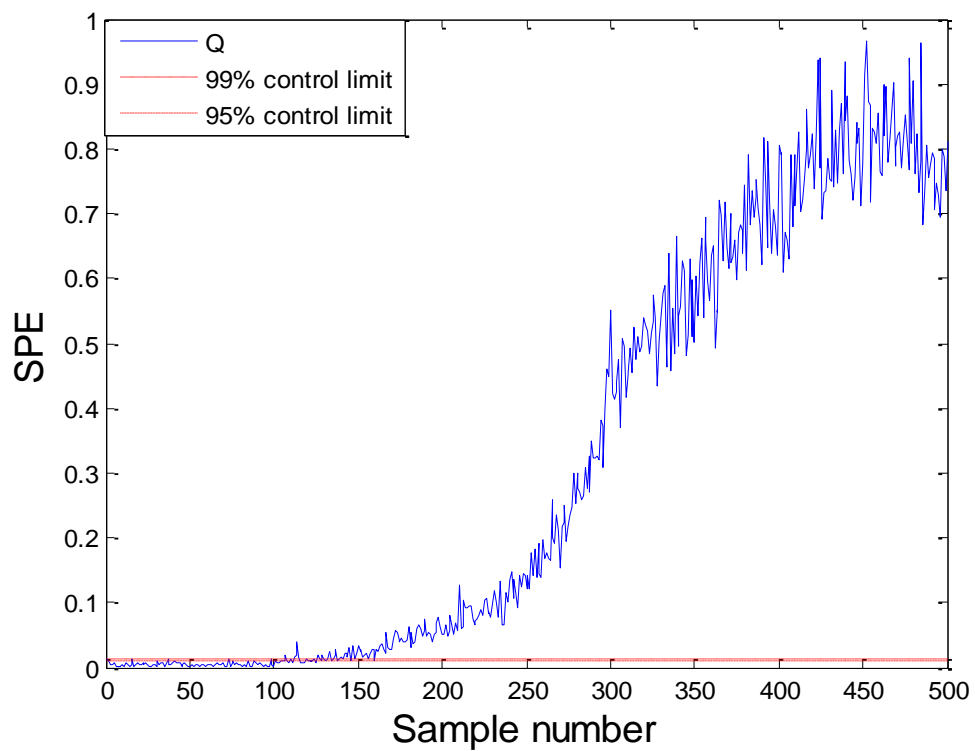
Figure 15

The difference between the E-AANN input and output; the input data had a drift error.

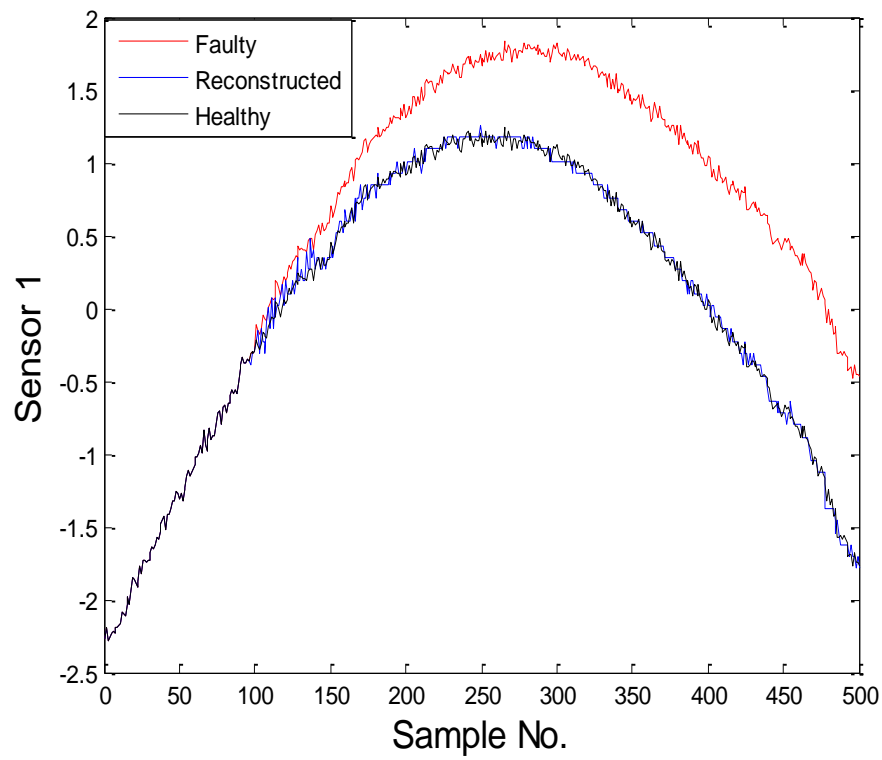
**Figure 16**

The mean of the difference between the input and output of the E-AANN for a drift fault.

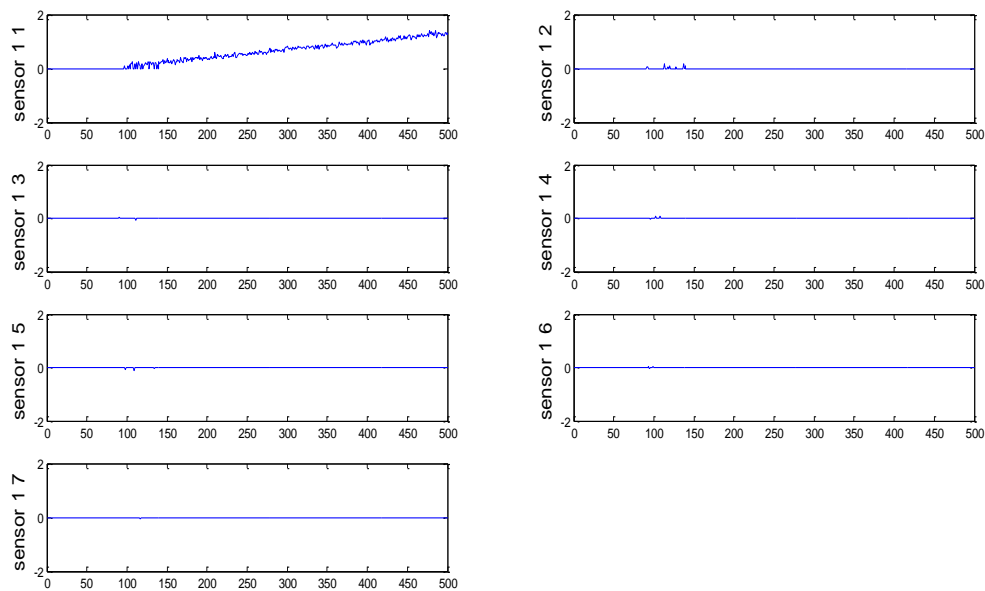
Figures 17–20 present the results of the I-AANN.

**Figure 17**

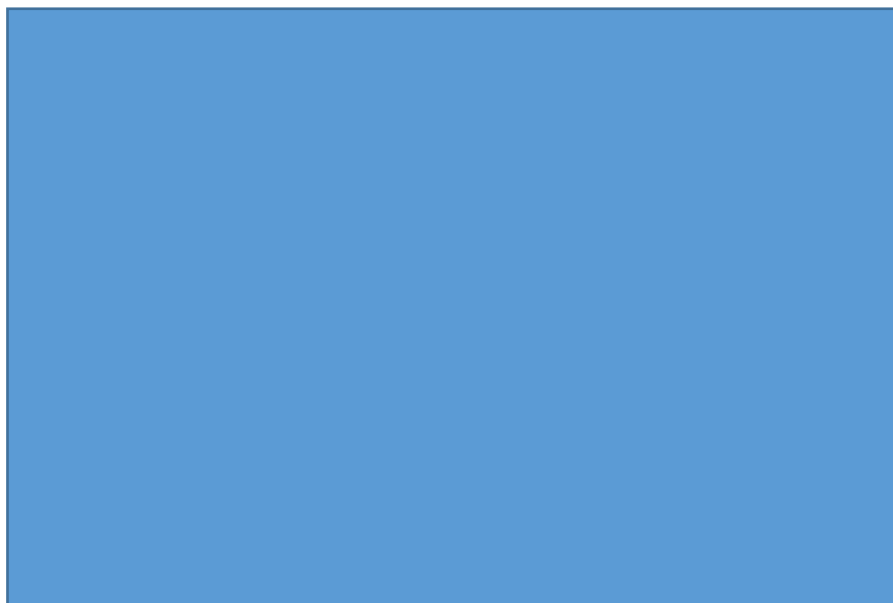
The drift fault detection by the I-AANN.

**Figure 18**

Sensor 1 output before contamination, after inducing a drift error, and after the reconstruction by the I-AANN.

**Figure 19**

The difference between the I-AANN input and output; the input data had a drift error.



7. Conclusions

The recently developed E-AANN algorithm has high computational time to isolate and reconstruct a single faulty sensor with a high degree of accuracy; hence, we have proposed a new algorithm named improved AANN, which has a high degree of accuracy and low computational time. The two algorithms were compared using a dimerization process. Both algorithms could detect and isolate the single faulty sensor properly, but the I-AANN had higher performance. Further, the I-AANN could isolate two sequential faulty sensors properly. The I-AANN is expected to be capable of online implementation for related future research. It can be developed for multiple-fault conditions and be compared with other fuzzy or neural network models.

Acknowledgments

This research paper is supported by the National Iranian Oil Company (NIOC) and Iranian Offshore Oil Company (IOOC).

Nomenclatures

A_K	The concentration of catalyst in the feed
AANN	Auto-associative neural network
B_c	The concentration of produced butene
E-AANN	Enhanced auto-associative neural network
FDI	Fault detection and isolation
F_e	Feed flow rate
I-AANN	Improved auto-associative neural network
NLPCA	Nonlinear principal component analysis
PCA	Principal component analysis
SPM	Statistical process monitoring

T	Reactor temperature
T_f	Feed temperature
W_c	Coolant flow rate
β	Recycle ratio

References

- Ali, E., and Al-humaizi, K., Advanced Control of Ethylene to Butene-1 Dimerization Reactor, Automatic Control and System Engineering, 2004.
- Borgan, T. R., Condition Monitoring Based on “Black-box” and First Principal Models, M.S.Dissertation, Dept. Cyber. Eng. Norwegian University of Science and Technology, 2011.
- Khaled, O., Fault Detection and Localization with Neural Principal Component Analysis, 18th Mediterranean Conference on Control & Automation Congress Palace Hotel, Marrakech, Morocco, June 23–25, 2010.
- Kramer, M.A., Nonlinear Principal Component Analysis Using Auto-associative Neural Networks. AIChE Journal, 1991, DOI:10.1002/AIC.690370209
- Najafi, Massieh (2003). Use of Auto-associative Neural Networks for Sensor Diagnostics. Master's thesis, Texas A&M University, Texas A&M University, Available electronically from <https://hdl.handle.net/1969.1/1392>.
- Najafi, M. Ch., Langari, Culp And R. Enhanced Auto-associative Neural Networks for Sensor Diagnostics (E-AANN), Proceedings of IEEE International Conference on Fuzzy Systems, 2004.
- Sing, H., Development & Implementation of an Artificially Intelligent Search Algorithm for Sensor Fault Detection Using Neural Networks, M.S. dissertation, Dept. Mech. Eng., Texas A&M University, 2004.
- Venkatasubramanian, E., Rengaswamy, R. Yin, K., Kavuri, S., N., A Review of Process Fault Detection and Diagnosis Part I: Quantitative Model-based Methods. Computers and Chemical Engineering, Vol. 27, p. 293–311, 2003.